

# The D $\rightarrow$ X Transition in $^{136}\text{Xe}^{19}\text{F}$

by

Katherine Johnson and Joel Tellinghuisen

Department of Chemistry

Vanderbilt University

Nashville, Tennessee 37235

## Abstract

The D ( $1/2^2P_{1/2}$ )  $\rightarrow$  X ( $2^+$ ) transition in XeF is recorded at high resolution for the single isotopomer  $^{136}\text{Xe}^{19}\text{F}$ , and the 0-0, 0-1, 0-2, and 1-2 bands are analyzed rotationally. The derived spectroscopic constants for the X state are in essential agreement with an earlier analysis of the B ( $1/2^2P_{3/2}$ )  $\rightarrow$  X system for this same isotopomer. The main new results for the D state are (units  $\text{cm}^{-1}$ ):  $T_e = 38055.13(10)$ ,  $\nu_e = 349.56(3)$ ,  $\nu_{ex_e} = 1.899(7)$ ,  $B_e = 0.160513(34)$ ,  $\nu_e = 1.247(7) \times 10^{-3}$ ,  $R_e = 2.5101(3) \text{ \AA}$ , (dimensionless spin splitting parameter) =  $-0.82(2)$ .

## 1. Introduction

The diatomic rare gas halides (RgX) were an instant "hit" in 1975, when the first RgX excimer laser was reported [1]. Most of the possible RgX species formed from Rg = Xe, Kr, and Ar could be observed in emission in high-pressure discharges, and many of these were made to lase [2,3]. XeF was quickly distinguished as unique among these molecules for the complexity of its emission spectrum. Like the others, it exhibited two prominent electronic bands, both confined to relatively narrow wavelength regions. However, whereas these bands proved to be mostly structureless at high resolution in the other RgX species, in XeF both of these, now known as the B<sup>1</sup>Σ<sup>+</sup> ← X<sup>1</sup>Σ<sup>+</sup> and D<sup>1</sup>Σ<sup>+</sup> ← X<sup>1</sup>Σ<sup>+</sup> transitions, revealed a mix of red- and violet-degraded band heads. This was a clear tip-off that these transitions were discrete, or bound-bound, in XeF, whereas they were bound-free in most of the other RgX species.

The complex band structure in the B<sup>1</sup>Σ<sup>+</sup> ← X<sup>1</sup>Σ<sup>+</sup> and D<sup>1</sup>Σ<sup>+</sup> ← X<sup>1</sup>Σ<sup>+</sup> systems of XeF was interpreted successfully soon after the XeF laser was reported [4-8]. However, efforts to interpret the rotational structure were frustrated by the abundance of isotopic Xe species present in natural Xe, which, through isotopic shifting, serve to blend most of the rotational structure to obscurity. A fortuitous cancellation of isotope effects made possible an analysis of a single band (the 1-2 band) in the B<sup>1</sup>Σ<sup>+</sup> ← X<sup>1</sup>Σ<sup>+</sup> system [8], which supported the theoretical model derived to account for the complex band contours. Monts *et al.* [9] got around the isotope problem by recording laser excitation spectra at high resolution in a free-jet expansion. For the '0' and '-1' bands of their study, the vibrational isotope shifts were large enough to permit separate analyses of the rotational structure for several isotopomers. Later we reported the B<sup>1</sup>Σ<sup>+</sup> ← X<sup>1</sup>Σ<sup>+</sup> emission spectrum for the single isotopomer <sup>136</sup>Xe<sup>19</sup>F in a Tesla discharge, and rotationally analyzed 13 '- '' bands [10].

The two extensive rotational analyses of refs. [9] and [10] were in overall agreement but nonetheless yielded statistically discordant results for the rotational constants of both states. The laser-excitation study was restricted to only small  $J$  values ( $J < 19/2$ ), because of the very low rotational temperatures in the free-jet expansion. This was not a problem in the single-isotope emission study.

On the other hand, the least-squares fits of the assigned lines in [10] had to be restricted to  $N'' \leq 40$ , because inclusion of higher levels led to systematic deviations for the Hamiltonian expressions used in that analysis. It was suggested that these effects might be due to perturbative interactions between the B and the C ( $^3/2 \ ^2P_{3/2}$ ) ion-pair states. However, the possibility of anomalies in the X state could not be ruled out.

To help resolve this issue, we have now examined the rotational structure in the D – X spectrum, which to our knowledge has never been rotationally analyzed. The D state is energetically far enough above the B and C states to ensure that its rotational level structure should be free of the postulated perturbations in the B state. Thus the observation of similar problems in the D – X spectrum would point to limitations in the X-state Hamiltonian. Of course the D – X transition is of interest in its own right. For example, the D – X system offers a potentially useful probe of X-state populations in dynamics studies [11,12]. Also, lasing has recently been demonstrated on the D – X transition in Ar and Ne matrices [13,14].

## 2. Experimental

The emission spectra analyzed here were recorded in the same way as were the B – X bands that were analyzed in [10]. The Tesla discharge sources contained 1-1.5 torr SF<sub>6</sub>, 2-3 torr <sup>136</sup>Xe (Mound Laboratory, 95.2% isotopic purity), and 140-170 torr Ar. The D – X emission was photographed in the region 2600–2660 Å on a 1.5-m JY HR-1500 spectrometer equipped with a 3600-groove/mm holographic grating (reciprocal dispersion 1.75 Å/mm, resolving power  $2 \times 10^5$ ). The slit width was nominally 5 μm, necessitating exposures of ~15 min on the Kodak IIA-O plates. The spectra were calibrated with Fe emission spectra from a microwave discharge source and were processed using the microdensitometer/microcomputer system described in other recent studies from this laboratory [15,16]. We estimate that sharp unblended lines in our spectra are measured with an absolute accuracy of  $\pm 0.04 \text{ cm}^{-1}$ .

### 3. Theoretical Summary

In the model developed in [7] to interpret the band structure in the B X and D X transitions, the X state is essentially a Hund's case b  $2^+$  state, while the B and D states are better thought of as Hund's case c  $= 1/2$  states. Thus the rotational levels in the X state group in accord with the rotational quantum number  $N$ , with only small spin splitting for the two  $J$  values associated with each  $N$  value. However, centrifugal distortion is very significant in the shallow, anharmonic X-state well, so it is necessary to include several higher-order centrifugal distortion terms in the expression for the energy. In the present work we have expressed the X-state rotational energies as

$$F_{e,f''}(N'',N'') = B'' e_{f''} - D''(e_{f''})^2 + H''(e_{f''})^3 + L''(e_{f''})^4 + M''(e_{f''})^5 \quad (1)$$

with

$$e'' = N''(N''+1) + N'' \quad (2)$$

$$f'' = N''(N''+1) - (N''+1).$$

The highest-order coefficients in Eq. (1),  $L''$  and  $M''$ , were assessed computationally [17], using an RKR potential derived from the X-state spectroscopic parameters obtained in [10]. Both of these terms make non-negligible contributions to the energy for the highest  $N''$  levels included among our assignments. In the final stages of our analysis, the  $H''$  values were also fixed at their computed values, as is discussed further below. The previous studies have yielded values of the spin-splitting parameter around  $-0.05$  for low  $N''$  levels.

The rotational levels of the B and D ion-pair states follow no simple pattern based on either their  $N$  or their  $J$  quantum numbers. However, the treatment by Kopp and Hougen [18] of the  $2^+$  and  $2^-$  molecular states correlating with an isolated  $1S + 2P$  atomic pair accounted nicely for the band contours in both the B X and D X systems analyzed in [7]. This model remains essentially valid at the more demanding level of the B-state rotational analysis [9,10]. Thus we anticipate that it should properly describe the levels in the D state. Accordingly the energies are expressed as

$$F_{e,f'}(N',J') = B' e_{f'} - D'(e_{f'})^2 \quad (3)$$

with

$$e_{e,f}' = J'(J'+1) - 1/2 \mp B'(J'+1/2). \quad (4)$$

It is worth recalling that the B and C states correlate with  $F^-(^1S) + Xe^+(^2P_{3/2})$ , while D arises from  $F^-(^1S) + Xe^+(^2P_{1/2})$  [hence the notation  $D(^{1/2} \ ^2P_{1/2})$ , for example]. For all of these ion-pair states, terms higher than second order in  $B'$  make negligible contributions to the energies in the present study. Furthermore, for low  $J'$  levels the  $D'$  values can be reliably calculated using the Dunham expressions for  $D_e$  and  $B_e$  [19]. Assuming that the B, C, and D states interact only among themselves ("pure precession"), theory predicts that  $B' + D' = 1$ . The actual theoretical estimates in [7] were  $B' = 1.87$  and  $D' = -0.87$ . For  $J' = 0$  and 1 of the B state, the experimental estimates from [10] were  $\sim 1.84$ , so we anticipate a value around  $-0.84$  for low  $J'$  levels in the D state.

When  $B' = -1.0$ , Eqs. (1-4) show that lines in the  $P_e$  branch coincide with those in the  $R_f$  branch having the same  $N$ , i.e.,  $P_e(N) = R_f(N)$ . For values of  $B'$  near  $-1.0$ , these two branches still march in lockstep, while at the same time the  $P_f$  and  $R_e$  branches take on the appearance of "super" P and R branches [7]. Furthermore, centrifugal distortion can lead to a "piling up" of the lines in the  $R_e$  branch. The end result is that the  $P_e$  and  $R_f$  branches may show many blends, while the  $R_e$  branch can be so congested so as to permit of few unique assignments. These points are illustrated in the Fortrat diagram of the 0-2 band shown in Fig. 1.

#### 4. Results and Discussion

Cognizant of the line congestion problems illustrated in Fig. 1, we focused our attention initially on  $J' - J''$  bands that were expected to be free at least of overlap with other  $J' - J''$  bands. The 0-2 band is ideal in this regard (see Fig. 2 in [8]). Because of line congestion and low intensity at low  $N$ , it was not possible to follow the branches back to the band origin. However it was easy to identify the  $P_f$  branch and (collectively) the  $P_e$  and  $R_f$  branches. There are inherent numbering ambiguities in such an analysis of a single band. However, these were resolved when we included the 0-1 band in the analysis, with a single set of rotational constants describing the upper state.

Extension to the 1-2 band was then straightforward, and we were eventually able to include many assignments in the 0-0 band as well. In the last case, there is extensive overlap with the 1-2 band, which appears to be dominant where the two bands overlap in our spectra. Consequently, in the overlap region we assigned to the 0-0 band only lines which were not already assigned to the 1-2 band. The assignments are summarized in Table 1, together with the band origins from a global fit of the data. Figure 2 illustrates a representative portion of the 0-1 band, which is the most completely assigned of the four bands.

The results of a least-squares (LS) fit to upper- and lower-state energies and level-by-level spectroscopic constants are given in Table 2. The LS estimates of the  $H''$  constants were statistically consistent with the RKR-based computed values, so the latter were adopted in the final fit. This was not true for the  $D''$  values, so the fitted results are given in this case. (In particular, the value for  $v'' = 1$  is many sigma larger than the calculated value of  $7.32 \times 10^{-7} \text{ cm}^{-1}$ , although the other two values are in reasonable agreement.) The  $B''$  and  $D''$  values exhibit very high mutual correlation, but are determined precisely relative to any member of the set. To emphasize this point, the statistical errors quoted for these parameters in Table 2 are those obtained after  $B_0$  was fixed at its LS value.

There was no indication of systematic behavior in the LS residuals from the final global fit. Since the assignments now extend to  $N'' = 87$ , well beyond the limit of 40 imposed on the LS fits of [10], it now seems very likely that the systematic errors at high  $N''$  in [10] were indeed due to deficiencies in the B-state Hamiltonian. This means that the B-X data will require a deperturbation analysis for extraction of the true mechanical parameters for the two states.

The two  $B'$  estimates of Table 2 lead to the  $B_e'$  and  $r_e'$  values quoted in the Abstract. The resulting value for the internuclear distance  $R_e$  in the D state is  $2.5101(3) \text{ \AA}$ . This value is remarkably close to the estimate of  $2.513 \text{ \AA}$  in [8], which was based entirely on band contour simulations and Franck-Condon intensity calculations.

A linear representation is inappropriate for the three  $B''$  values because of the very nonlinear dependence of these on  $v''$  [10]. Alternatively, we compare in Fig. 3 the results of the present

determination with those of Refs. [9] and [10]. Although two of the three present  $B''$  values differ by more than 1 from those calculated from the parameters in Table II of [10], the discrepancies are small enough to be within the limitations of the earlier analysis, now that it seems likely that the B-state levels are perturbatively mixed with the C state. On the other hand the present values are not statistically consistent with the values obtained in [9].

The values of the spin-splitting parameter  $\lambda''$  are thought to be better determined than in the earlier B-X analysis [10], because of the much greater range of  $N''$  covered by the assignments. The new values are larger in magnitude by an amount that is within the combined standard errors in the two determinations (e.g.  $-0.0777$  vs the previous  $-0.0567$  for  $\lambda'' = 0$ ). As was noted in the B-X analysis, the quantity which is actually precisely determined for a given band is the sum ( $B' + B''$ ). For example, in one test fit  $\lambda_0''$  was fixed at the earlier value, leading to parallel changes in the other  $\lambda''$  values and a concomitant increase in the magnitudes of the two  $\lambda''$  values (to  $-0.8490$  and  $-0.8418$ ). (In this fit there was also an increase by  $2 \times 10^{-5} \text{ cm}^{-1}$  in all of the  $B$  values, and the variance rose by a nominal 0.5%.) Because of the strong negative correlation between  $\lambda''$  and  $\lambda_0''$ , we recommend that users of the B-X results in [10] stick with those X-state parameters until such time as the B-X system can be deperturbed and combined with the D-X data in a consistent global determination of all three states.

The band origins from Table 1, appropriately weighted, were combined with the estimated origins given in Table IV of [8] and were fitted to the usual double polynomials in  $(v'' + 1/2)$  and  $(v'' + 1/2)$  to extract improved estimates of the vibrational parameters for the D state. In this determination, the data from [8] were assigned an average isotopic mass of 131.3, the same procedure as was followed in [10]. The results of this analysis are given in Table 3. It should be noted that in the course of the current study it became apparent to us that there existed a calibration inconsistency between the D-X spectrum which was analyzed in [10] and the present results. Since our current spectra were obtained in multiple exposures which appear fully consistent in their region of overlap, we have concluded that there was a calibration error in the earlier spectrum. In the

present work we have taken this into account by including a calibration correction parameter, taken to be a simple constant shift in the wavelength. The fitted value of this shift is included in Table 3. The main consequence of the correction is an increase in  $T_e$  for the D state by  $3.7 \text{ cm}^{-1}$ .

The strong anharmonicity of the X state means that the vibrational parameters for it in Table 3 cannot be compared quantitatively with the earlier determinations, because the  $v''$  ranges spanned by the data, and hence also the optimal number of parameters, were different. However, we can compare our X-state energies with those from [10]. This comparison is not entirely satisfactory. In particular, the first interval ( $G_0''$ ) from the present study is smaller by  $0.043 \text{ cm}^{-1}$  and the second ( $G_1''$ ) is larger by  $0.195 \text{ cm}^{-1}$ . These discrepancies, while not significant for most practical applications, are nonetheless far outside the combined statistical errors. They also greatly exceed our estimates of possible calibration errors. The source of the disparities cannot be ascertained at present and will have to be addressed in future work on the two systems.

## 5. Conclusion

The D  $\rightarrow$  X spectrum of  $^{136}\text{Xe}^{19}\text{F}$  has been recorded at high resolution from a Tesla discharge source, and four  $v'' - v''$  bands have been rotationally analyzed. The analysis yields the first precise spectroscopic information about the D state of XeF. The results for the X state largely corroborate an earlier study from this laboratory of the B  $\rightarrow$  X transition for this same isotopomer [10] but are not in satisfactory agreement with the only other existing high-resolution study of this molecule [9]. An indirect consequence of this study is support for the earlier suggestion that systematic errors for  $N'' > 40$  in the B  $\rightarrow$  X transition [10] are likely due to perturbations between B- and C-state levels. These perturbations probably involve coriolis coupling, and should be amenable to the same kind of deperturbation treatments that have been applied successfully to ion-pair states in the halogens [20].

## Acknowledgment

This work was supported by the National Science Foundation under Grant CHE-8910823.

## References

- [1] S. K. Searles and G. A. Hart, *Appl. Phys. Lett.* 27 (1975) 243.
- [2] C. A. Brau, *Top. Appl. Phys.* 30 (1979), 87.
- [3] E. W. McDaniel and W. L. Nighan, eds. *Applied Atomic Collision Physics: Vol. 3 – Gas Lasers* (Academic Press, New York, 1982).
- [4] J. Tellinghuisen, G. C. Tisone, J. M. Hoffman, and A. K. Hays, *J. Chem. Phys.* 64 (1976) 4796.
- [5] J. E. Velazco, J. H. Kolts, D. W. Setser, and J. A. Coxon, *Chem. Phys. Lett.* 46 (1977) 99.
- [6] A. L. Smith and P. C. Kobrinsky, *J. Mol. Spectrosc.* 69 (1978) 1.
- [7] J. Tellinghuisen, P. C. Tellinghuisen, G. C. Tisone, J. M. Hoffman, and A. K. Hays, *J. Chem. Phys.* 68 (1978) 5177.
- [8] P. C. Tellinghuisen, J. Tellinghuisen, J. A. Coxon, J. E. Velazco, and D. W. Setser, *J. Chem. Phys.* 68 (1978) 5187.
- [9] D. L. Monts, L. M. Ziurys, S. M. Beck, M. G. Liverman, and R. E. Smalley, *J. Chem. Phys.* 71 (1979) 4057.
- [10] P. C. Tellinghuisen and J. Tellinghuisen, *Appl. Phys. Lett.* 43 (1983) 898.
- [11] H. Helm, L. E. Jusinski, D. C. Lorents, and D. L. Huestis, *J. Chem. Phys.* 80 (1984) 1796.
- [12] J. F. Bott, R. F. Heidner, J. S. Holloway, J. B. Koffend, and M. A. Kwok, *J. Phys. Chem.* 93 (1989) 4060.
- [13] H. Kunttu, W. G. Lawrence, and V. A. Apkarian, *J. Chem. Phys.* 94 (1990) 1692.
- [14] G. Zerza, G. Sliwinski, Nd N. Schwenter, *Appl. Phys A56* (1993) 156.
- [15] P. C. Tellinghuisen, B. Guo, D. K. Chakraborty, and J. Tellinghuisen, *J. Mol. Spectrosc.* 128 (1988) 268.
- [16] M. A. Stepp, M. Adam Kremer, P. C. Tellinghuisen, and J. Tellinghuisen, *J. Mol. Spectrosc.* 146 (1991) 169.
- [17] J. Tellinghuisen, *J. Mol. Spectrosc.* 122 (1987) 455.
- [18] I. Kopp and J. T. Hougen, *Can. J. Phys.* 45 (1967) 2581.

[19] G. Herzberg, *Spectra of Diatomic Molecules* (Van Nostrand, Princeton, 1950).

[20] J. C. D. Brand and A. R. Hoy, *Appl. Spectrosc. Rev.* 23 (1987) 285.

### Figure Captions

- Figure 1: Fortrat diagram for the 0-2 band of the D<sub>2</sub> - X transition in  $^{136}\text{Xe}^{19}\text{F}$ .
- Figure 2: A segment of the D<sub>2</sub> - X spectrum (densitometer trace) of  $^{136}\text{Xe}^{19}\text{F}$  in the region of the 0-1 band, with calculated positions of lines in the four branches (labeled by  $N''$ ) indicated above.
- Figure 3: Comparison of present estimates of  $B$  for  $v = 0-2$  in the X state of  $^{136}\text{Xe}^{19}\text{F}$  with results from previous studies. In each case the plotted quantity is the indicated value minus the value calculated using the constants in Table II of [10]. For the present results, the error bars ( $1\sigma$ ) are roughly the size of the plotted points. For the purpose of this comparison, the isotope relations [19] have been used to calculate values for  $^{136}\text{Xe}^{19}\text{F}$  from the parameters given for  $^{131}\text{Xe}^{19}\text{F}$  in Table I of [9].

Table 1

Summary of bands included in rotational analysis of the D – X transition in  $^{136}\text{Xe}^{19}\text{F}$

$v' - v''$	$\nu_0$ (cm $^{-1}$ ) <sup>a</sup>	$N''$ Range <sup>b</sup>
0–0	38 120.695 (18)	16–71 (78)
0–1	37 917.143 (16)	18–87 (139)
0–2	37 733.874 (11)	12–65 (105)
1–2	38 079.637 (15)	18–67 (95)

<sup>a</sup>Band origins from least-squares analysis, with 1- $\sigma$  error in parentheses, in terms of final digits.

<sup>b</sup>Numbers of assignments given in parentheses.

Table 2

Spectroscopic parameters ( $\text{cm}^{-1}$ ) for analyzed vibrational levels in the D and X electronic states of  $^{136}\text{Xe}^{19}\text{F}^a$

level	$T_0^b$	$B$	$\delta, c$	$10^7 \times D$	$10^{11} \times H^{d,e}$
" = 0	0	0.187 377 (39)	-0.0777 (9)	6.08 (4)	-0.700
" = 1	203.554 (23)	0.181 607 (35)	-0.0778 (6)	7.44 (1)	-1.216
" = 2	386.822 (21)	0.174 814 (35)	-0.0797 (9)	9.02 (3)	-2.242
' = 0	38 120.695 (18)	0.159 890 (34)	-0.8250	1.361 <sup>d</sup>	0
' = 1	38 466.458 (23)	0.158 643 (34)	-0.8179 (13)	1.362 <sup>d</sup>	0

<sup>a</sup>Figures in parentheses represent 1- errors, in terms of final digits.

<sup>b</sup>Energies relative to " = 0 in the X state.

<sup>c</sup>Spin-splitting constants; see text. The stated errors are those obtained when ' = 0 is fixed at the indicated value, breaking the strong correlation among these parameters, all of which are otherwise uncertain by  $\sim 0.015 \text{ cm}^{-1}$ .

<sup>d</sup>Parameters fixed at indicated values; see text.

<sup>e</sup>Higher-order centrifugal distortion parameters fixed in analysis (units  $\text{cm}^{-1}$ ):  $L_0'' = -2.11 \times 10^{-16}$ ,  $L_1'' = -4.39 \times 10^{-16}$ ,  $L_2'' = -1.11 \times 10^{-15}$ ,  $M_0'' = -0.80 \times 10^{-20}$ ,  $M_1'' = -2.29 \times 10^{-20}$ ,  $M_2'' = -6.95 \times 10^{-20}$ .

Table 3

Vibrational parameters (cm<sup>-1</sup>) for the D X transition in <sup>136</sup>Xe<sup>19</sup>F<sup>a,b</sup>

	D (1/2)	X (2 <sup>+</sup> )
$c_0 (T_e)$	38 055.13 (10)	
$c_1 (e)$	349.56 (3)	221.84 (26)
$c_2 (-eXe)$	-1.899 (7)	-8.51 (22)
$c_3 (eYe)$		-0.417 (66)
$c_4$		0.017 (6)
		1.77 <sup>c</sup>
range	0–12	0–6

<sup>a</sup> From fit of band origins in Table 1 and low-resolution data from Table IV of Ref. [8]. The fitted wavelength correction for the latter was -0.347(12) Å.

<sup>b</sup> Standard errors (1  $\sigma$ ) in parentheses.

<sup>c</sup> Standard deviation for data of unit weight in Table IV of Ref. [8].

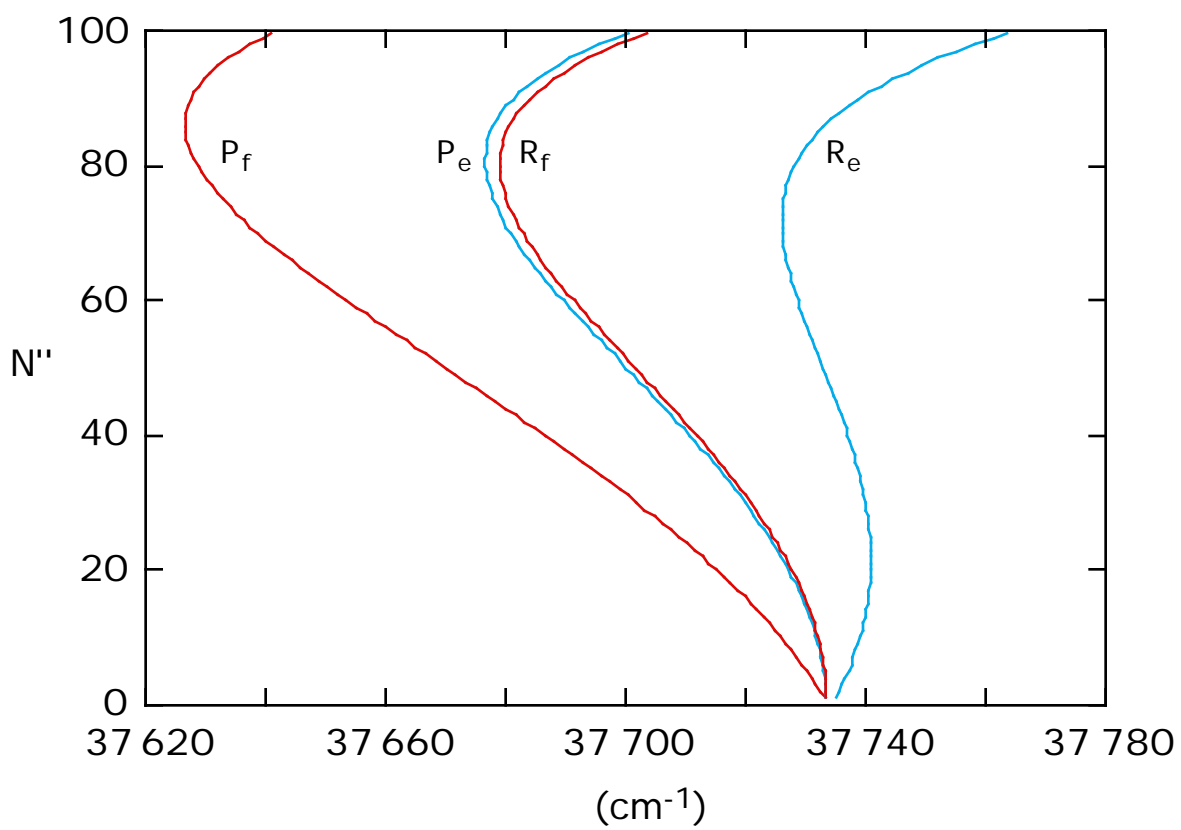


Figure 1: Fortrat diagram for the 0-2 band of the D-X transition in  $^{136}\text{Xe}^{19}\text{F}$ .

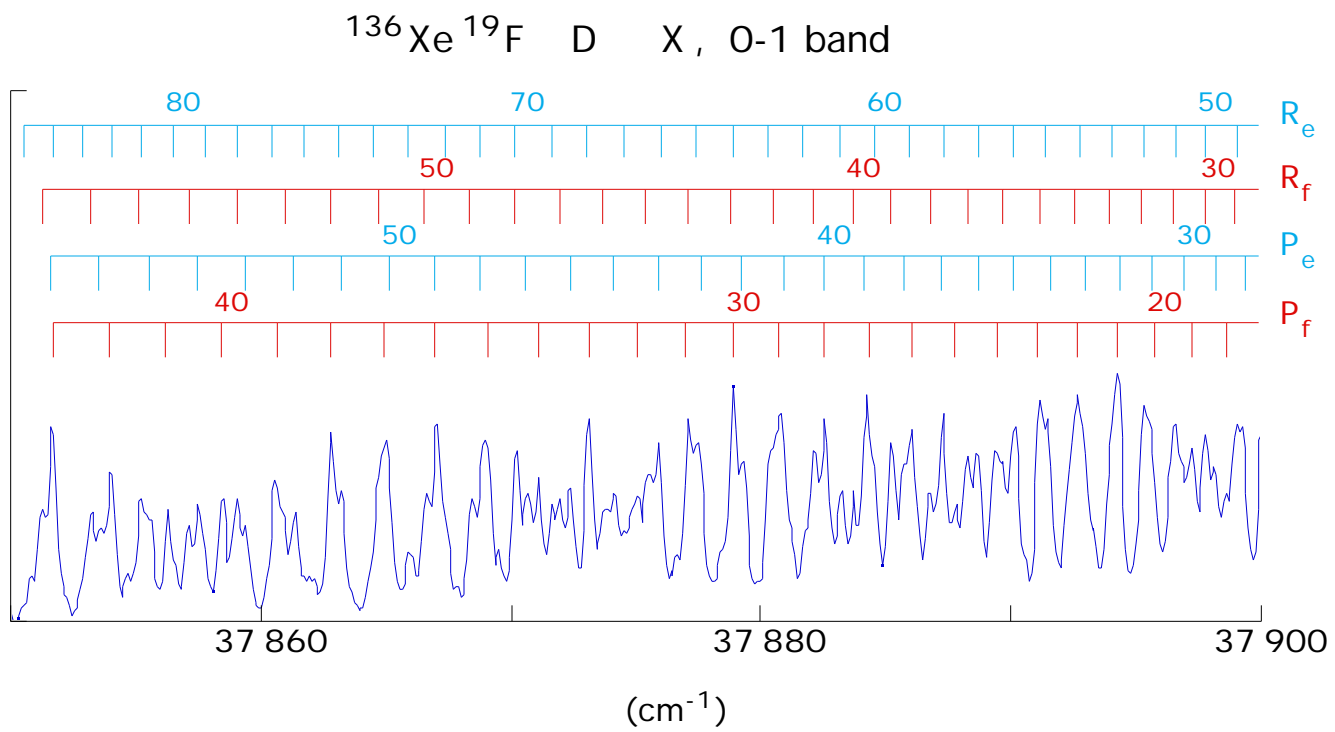


Figure 2: A segment of the D X spectrum (densitometer trace) of  $^{136}\text{Xe}^{19}\text{F}$  in the region of the 0-1 band, with calculated positions of lines in the four branches (labeled by  $N''$ ) indicated above.

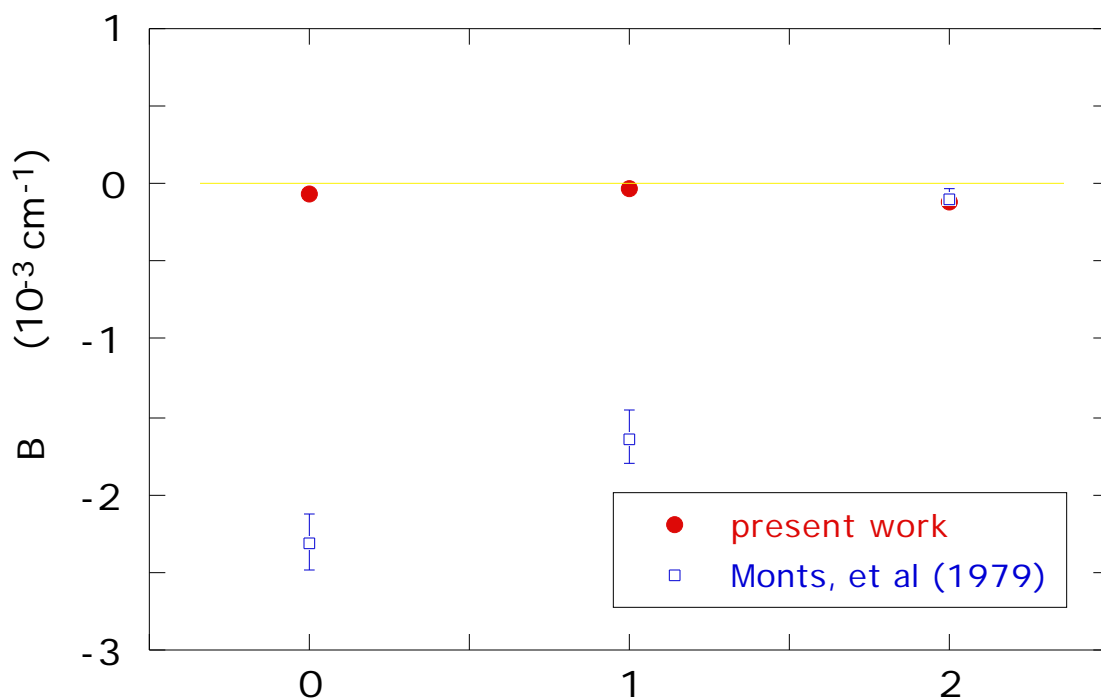


Figure 3: Comparison of present estimates of  $B$  for  $J = 0-2$  in the X state of  $^{136}\text{Xe}^{19}\text{F}$  with results from previous studies. In each case the plotted quantity is the indicated value minus the value calculated using the constants in Table II of [10]. For the present results, the error bars (1  $\sigma$ ) are roughly the size of the plotted points. For the purpose of this comparison, the isotope relations [19] have been used to calculate values for  $^{136}\text{Xe}^{19}\text{F}$  from the parameters given for  $^{131}\text{Xe}^{19}\text{F}$  in Table I of [9].